

A Proposed Method for Measuring the Electric Dipole Moment of the Neutron Using Acceleration in an Electric-Field Gradient and Ultracold Neutron Interferometry

M. S. Freedman,^{1*} G. R. Ringo,¹ and T. W. Dombeck²

¹*Argonne National Laboratory, Argonne, IL 60439*

²*Fermilab, Batavia, IL 60510*

(April 29, 2019)

Abstract

The use of an ultracold neutron interferometer incorporating an electrostatic accelerator having a strong electric field gradient to accelerate neutrons by their possible electric moments is proposed as a method of measuring the neutron electric dipole moment. Such electrical acceleration, followed by an amplifier and a generator of phase difference, could develop relatively large phase differences and these could be measured by a Mach-Zehnder interferometer. This method might extend the sensitivity of the measurement by several orders of magnitude beyond the current limit of 10^{-25} e.cm. Furthermore the systematic errors in such a measurement could be significantly different from those of the current EDM experiments.

PACS Codes: 06.30.Lz, 07.60.Ly, 13.40.Em, 14.20.Dh

Key Words: electric, moment, interferometry, neutron

Contents

I	Introduction	3
II	The Proposed Instrument	4
	A Principle of Operation	4
	B The Proposed Open-Box Accelerator	6
	C Phase Difference Generation	8
	D The Assembly	10
III	Comparison to the Precession Method	12
IV	Problems	12
	A The $\mathbf{v} \times \mathbf{E}/c^2$ Effect	13
	B Magnetic Fields	14
	C Reflectivity	17
	D Leakage Currents and Surface Charges	17
	E Precision and Stabilization	18
	F Gravitational and Sagnac Effects	18
	G Decoherence	18
	H Control, Calibration and Alignment Measurements	18
V	Simplified Test of the Operating Principles	19
VI	Other Interferometers	20
VII	Conclusions	21

I. INTRODUCTION

The existence of a neutron electric dipole moment (EDM) would demonstrate the violation of time reversal invariance. The measurement of the EDM is one of the most sensitive time reversal tests available. The experimental searches for the EDM by the method of Norman Ramsey and his colleagues [1,2] have increased in sensitivity by a factor of about 10^5 beyond their first measurement which was itself quite a sensitive test. Most measurements of the neutron EDM have been NMR measurements [1,2,3] in which one looks for the effect of a strong electric field on the precession rate of the neutron spin. To enhance sensitivity all such recent measurements are made with ultracold neutrons (UCN; $T < 3\text{mK}$) which can precess for long times while stored in containers made of materials which reflect them coherently, even at normal incidence. Only one other measurement, by Shull and Nathans [4], was not done by an NMR measurement. In 1967 they set a limit of about 7×10^{-22} e.cm for the EDM (expressed in the usual fashion of the electron charge times the separation of electrons of opposite charge, needed to give the measured moment). They looked for the effect of the strong electric field gradients in atoms on the EDM via the imaginary term in the neutron scattering amplitude of cadmium. However, the best current measurements [1,2] using the precession method give (95% CL) $\leq 10^{-25}$ e.cm for the EDM which is a factor of thousands lower than the Shull and Nathans experiment. In view of the importance of the EDM and the great delicacy of the measurements, it seems very desirable to have a test with different systematic errors and a sensitivity comparable to the Ramsey method. This paper describes a method which is not only different from the Ramsey method but could possibly provide higher sensitivity.

Measurement of the EDM by neutron interferometry was proposed by Anandan [5] in 1982. His method was to measure the uniformly accumulating phase shift of a polarized neutron placed in a strong uniform electric field along the spin axis. He did not claim significant gains in sensitivity over the precession method in which the neutron precesses in a plane orthogonal to the electric field. We are proposing a different interferometric method [6] which should give a considerable advance in sensitivity. No scheme can violate the time-energy uncertainty principle which limits $\Delta\epsilon \geq h/(\Delta t)$ for one neutron. The $\Delta\epsilon$ limit for Δt of the order of the neutron lifetime is currently approached by the precession method for an EDM limit of order 10^{-27} e.cm, but for our proposal the same $\Delta\epsilon$ corresponds to an EDM smaller by about 10 orders of magnitude (see Sect. II). Several proposals are the main themes of this paper. These are:

1. The amplitude of each UCN wave function (velocity ≤ 4.5 m/s for us; $\lambda \sim 100$ nm) would be split into two overlapping partial waves with spins parallel and antiparallel to a magnetic guide field. This scheme would maintain the partial waves coherence for long times while suppressing adventitious phase shifts. These partial waves are the “arms” of our interferometer. For this purpose we propose the use of UCN with their spins orthogonal to the magnetic guide field direction. This is described in Sect. II-A.
2. We would generate a velocity difference and thus a desirable (microscopic) spatial separation between the partial waves by a differential acceleration of their EDMs in an electric field gradient for long times, while retaining a significant range of UCN velocities in the electric gradient. These are accomplished in the “Open Box Accelerator”

with a dihedral ceiling, Sect. II-B.

3. We suggest two methods for converting the spatial separation into a greatly enhanced potential difference. Both produce a growing phase difference between the partial waves while conserving the UCN fluence. They are described in Sect. II-C, “Phase Difference Generation” and in Sect. II-D, “The Assembly” incorporating a drift space.
4. Finally, the phase difference is measured by a Mach-Zehnder interferometer in which the first reflector is a magnetized mirror which sends one spin state in one path and the other in the other path. One of the spin states is rotated π radians and they are put together at the recombiner.

We also present fairly detailed analyses of some significant sources of systematic error; in Sec. IV-A, “ $\mathbf{v} \times \mathbf{E}$ ”; in Sect. IV-B, “Magnetic Fields”; in Sect. IV-F, “Gravitational and Sagnac Effect”; and in Sect. IV-H, “Control, Calibration and Alignment Measurements”.

This proposal is clearly an optimistic extrapolation of a barely started technology which uses several untested ideas, in fact there has been significant theoretical criticism of our basic assumption, item 3 above. No one should embark on such a measurement without testing our assumptions on a small scale. In Sect. V we suggest relatively cheap ways of testing by measuring the well-known neutron magnetic moment using our proposed method.

The aim of this paper is to offer suggestions and not to make judgments as to matters of strategy, let alone engineering. All our numbers are to be taken as illustrative.

II. THE PROPOSED INSTRUMENT

A. Principle of Operation

Splitting the wave function amplitude of each particle in the beam is the first step in interferometers. The common way of doing this is by separating the partial waves geometrically. For us this would pose very difficult construction problems. Owing to the low phase space density of the UCN sources, we need to obtain UCN from broad, uncollimated polychromatic sources. We need to contain these neutrons for perhaps 10 minutes in apparatus of the order of 1 meter in size. We would have to make the two separated paths for each UCN identical to a few nm although the paths are multiply folded and kilometers long. In addition, slight differences in the vibration histories of the separate containers might be fatal.

A better way to separate the paths would be by their quantum states. This is relatively easy to arrange. The beautiful atomic interferometer measurement of the acceleration of gravity done by Kasevich and Chu [7] demonstrates that this technique is sound in principle and is practical. In our EDM scheme the spatial separation of the two states is of the order of nanometers at most and they are reflected simultaneously from nearly the same area at all times. It is not necessary, of course, to match the varied path lengths of different UCN.

All our computer modeling and our use of semi-classical equations of motion refer to point-like particles. The actual interactions of UCN with fields and media surfaces extend over regions at least the size of the UCN wavelength. There is ample precedent for the application of semiclassical methods in following the course of development of the quantum

mechanical properties of ensembles of particles, e.g. phase difference, in such billiard-like problems as ours [8].

We first consider a simple accelerator followed by a detector (Fig. 1) to introduce the main ideas of the scheme. We start with a pulsed beam of monochromatic UCN polarized in the direction they are moving (the x-direction) with a weak magnetic guide field in the x-direction. Applying an RF-field, at the Larmor frequency and normal to x, for a suitable time will rotate the spin to a direction normal to the x axis and it will start to precess around that axis. This state is equivalent to coherently superposed eigenstates of the magnetic field, one with spin parallel to x, the other anti-parallel. These constitute the two partial waves of our interferometer. We call this pair, “bipolarized”. This superposition has been demonstrated both experimentally and theoretically by Summhammer *et al.* [9] and by Badurek *et al.* [10]. In particular they showed that the separated coherent bipolarized neutron eigenstates, when recombined interferometrically, summed their independent phase shifts. These phase shifts correspond to polarization rotations, even from interactions which were not spin dependent.

The UCN flow through an electric field gradient in the x-direction for a time. There one spin state is accelerated by the force of the gradient acting on one electric dipole but the other state, of opposite spin and dipole moment, is decelerated. This leads to a growth of a phase difference, Δf , between the spin states. The UCN next pass into an RF coil parallel to the first coil which is then turned on at the same frequency and phase as the first RF coil. At this time, common to both spin states, the bipolarized state and its differential phase gain are terminated by applying that field for the same duration as the first. Thus the interference of the two spin states occurs after traversing equal-time arms as in Kasevich and Chu [7] and as in the Ramsey precession method [1,2,3] instead of equal-space length arms as in Mach-Zehnder particle interferometry.

The $\pi/2$ spin rotation induced by the second RF leaves it anti-parallel with the initial spin if there is no EDM and slightly off that if there is a polarization change dependent on the phase difference generated in the field gradient. (In practice the polarization change is more sensitive to the phase difference of the UCN states if the second RF is shifted by $\pi/2$ in phase relative to the first.) The polarization would be detected by standard means after the second RF field. All this is very similar to the precession measurement [1].

For the phase difference $\Delta\phi$ between the spin states generated in t_a seconds in the accelerator, we follow the development of Greenberger and Overhauser [11]. It is given by the line integral

$$\hbar\Delta\phi = \int_0^{t_a} (V_{\rightarrow} - V_{\leftarrow}) dt = \int_0^{t_a} \Delta V dt \quad (1)$$

where the potential energy difference between the states, labeled by the arrows, is a small perturbation on the free particle Hamiltonian. Since the fields between the RF spin flipper, the electric, magnetic and gravitational, are all static, total energy is conserved,

$$\Delta W = \Delta V + \Delta T = 0. \quad (2)$$

ΔT is the kinetic energy difference. Hence

$$\hbar\Delta\phi = \int_0^{t_a} -\Delta T dt. \quad (3)$$

For small Δv_x

$$-\Delta T = mv_x \Delta v_x \quad (4)$$

where Δv_x is the difference in velocity of the two spin states produced by the electric field gradient, and m is the neutron mass. (Here we are ignoring the relatively large guide field interaction with the magnetic moment, $2\mu_m B$, because it could be canceled, for example, by reversing the magnetic field non-adiabatically in mid course, or by other ways discussed in Sect. IV-B.) The force of the electric gradient on the dipole gives after t_a seconds

$$\Delta v_x = \frac{2\mu_e t_a}{m} \left(\frac{\partial E_x}{\partial x} \right). \quad (5)$$

Here the factor 2 accounts for two spin states, μ_e is the neutron EDM (arbitrarily assumed to be parallel to the spin vector) and E_x is the x-component of the electric field. We then have from (3), (4), and (5)

$$\hbar \Delta \phi = \mu_e t_a^2 \left(\frac{\partial E_x}{\partial x} \right) v_x. \quad (6)$$

In the precession method

$$\hbar \Delta \phi = 2\mu_e E_x t_P, \quad (7)$$

where t_P is the time spent in the electric field. The interferometer in Fig. 1 would, in practice, be far less sensitive than Refs. [1] and [3]. Monochromatization and pulsing would greatly reduce the number of UCN. Also the time in the gradient is very small compared to the times, t_P , of stored UCN. The above calculation makes the important point that the effect of the gradient is proportional to t_a^2 .

There are several ways of realizing a UCN interferometer with a large t_a . We will describe two, each consisting of an accelerator with a special UCN storage arrangement in order to gain the largest possible Δx , followed by an amplifier and a generator of phase difference. The latter are shown dashed in Fig. 1.

B. The Proposed Open-Box Accelerator

To hold the full UCN velocity range for a long time in the accelerator one might consider putting the transversely polarized UCN into a rectangular box of totally-reflecting optical flats, made of insulators, located in a static, uniform, longitudinal, electric-field gradient. For a given longitudinally polarized partial wave, after each spectral reflection from the walls perpendicular to the x direction of the polarization, the x-component of the velocity reverses relative to the acceleration which is unidirectional; it is well established that the polarization is conserved on reflection [2] and that UCN reflection is specular [12]. It is obvious that the reversal of the signs of $v_{x \rightarrow}$ and $v_{x \leftarrow}$ with preservation of their magnitudes on reflection at walls normal to the x-axis entails the reversal of their difference $\Delta v_x = v_{x \rightarrow} - v_{x \leftarrow}$. Thus the Δv_x gained in each traversal effectively cancels the Δv_x gained in the previous traversal of the box.

We considered a number of accelerator schemes that do not suffer such cancellation of Δv_x . By far the most favorable in overall system simplicity, size, cost, sensitivity, and minimization of systematic errors is the “open box” shown in Fig. 2. We propose to do the x-direction differential acceleration in an open box made of dielectric UCN-reflecting plates, say, 50 cm long in the y direction, by 10 cm (x) as floor; and having 2 ceiling plates each 5 cm wide in the x direction, joined at a small dihedral angle (~ 0.01 radians) in the z direction, peaked in the middle ($x = 0$). The box would be 5 cm high. Two 5 by 10 cm wall plates would close the y ends. The box would be open in the $\pm x$ directions to avoid wall reflections of v_x . Provided $v_z/v_x \sim 10$ or greater it is possible to reflect UCN of sufficiently broad, low-x-velocity range back and forth along the x coordinate without suffering the reversal of Δv_x indicated above. This is accomplished by several reflections from the tilted top plates in a manner described in the Appendix. This arrangement retains in the steep electric gradient region many more UCN (by 10^3 for $t_a = 100$ s) than would remain if the ceiling were flat.

A plausible, qualitative description of the processes in the open and closed boxes follows. Consider the bipolarized state being reflected back and forth from the dihedral ceiling and planar floor and moving towards $\pm x$, but without the electric field. Clearly both partial waves will reverse their x motion at exactly the same $|x|$ value, on the ceiling. Now with the electric field turned on its gradient will “pull” one polarization state towards the $+x$ direction to which it was aiming, and repel the other state away from that end, thus helping it turn around. Obviously, the latter (lagging wave \mathbf{v}_\leftarrow , in Fig. 9 of the Appendix) will reverse its x motion at smaller $|x|$ than the former. After the x motion reversal the leading and lagging waves interchange roles. Thus their Δv_x always preserves its sense with respect to the acceleration direction, i.e., $v_\rightarrow = v_\leftarrow + \Delta v$. In the case of the closed box, on the contrary, the leading wave reverses first on every x-reflection, thus reversing the sign of Δv_x , leading to its near cancellation. See the Appendix for further remarks.

In the horizontal direction UCN with a $|v_x|$ of 0.3 m/s in the center of the open box can be retained effectively with an optimal dihedral ceiling angle of about $|0.006|$ radians from the x axis according to our computer simulations. A complication is that most UCN with $v_z < 3$ m/s will not behave properly in the open box and will be lost. About 1% of all the UCN with $v < 4.5$ m/s can be retained for 100 seconds. The rest quickly escape and are absorbed on the vacuum walls.

Note that a shallow concave roof, either parabolic or circular, with an average slope matching that of the dihedral roof, $|0.006|$ rad, is even more effective in retaining low v_x UCN. However such concave curvatures counteract the electric differential acceleration (see Sect. II-C, “Convex Floor Amplifier”) so they cannot be used.

A static, hence energy conservative, electric field gradient (Fig. 3) would be supplied by four horizontal rod electrodes at least 0.6 m long in the y direction, arranged in a symmetrical diamond array; the pair in the yz plane opposite in polarity to the pair in the xy plane, the pair members spaced 50 cm apart (Fig. 2). (The electrodes in the xy plane, connected in a loop, could serve as the coil of an RF spin rotator for both the accelerator box and the drift space.) The gradient ($\partial E_x/\partial x$) varies only a few percent within the box along any direction. Along the x centerline plane of the box the electric field is zero (Fig. 3). Hence the electric polarization of the neutron induced by the weak field in the box is negligible, in view of the neutron’s very small polarizability [13] (0.9×10^{-31} e.cm in fields of 10^6 V/m). Moreover, induced polarization cannot contribute to the differential acceleration.

The dihedral ceiling and the floor, in practice, would be much wider in the x direction than 10 cm to minimize dielectric edge effects on field smoothness in the middle 10 cm as explained in Sect. IV-A. The dihedral angle should extend only to $|x| = 5$ cm, thus confining about 1/3 of the UCN with $|v_x| \leq 0.3$ m/s (at their entrance into the box) to this range. The dielectric mirrors should be optically smooth and polished but could tolerate surface waviness and misalignment at the one tenth milliradian level.

For each component of the bipolarized state the electric acceleration is nearly constant, unidirectional, independent of the sign of the small v_x and opposite that of the other spin component, and energy conservative. The orientation of $\Delta\mathbf{v}$ is nearly constant so Δv_x grows as t_a . The resulting spatial separations between the members of the partial wave pairs as they leave the accelerator, Δx_a , are nearly the same, within a few percent for all partial wave pairs, even though their $\langle \Delta\phi \rangle = 0$. On every traversal v_x , hence ΔT , hence $\Delta\phi$, all reverse, hence cancel; Eqs. (3, 4). Any variation in Δx_a would be due mainly to the small variation in the magnitude of the electric field x-gradient over the box which the UCN scan. It is the separation, Δx_a , of the partial wave packets rather than the velocity difference Δv_a from the accelerator, which leads in the converter-amplifier (Sect. II-C), to a large gain in average gravitational potential difference, which difference persists in the drift space.

Gravity causes all the trajectories in the accelerator and amplifier to be sections of vertical parabolas; the partial waves bounce together along the x and y coordinates, the pair members separating very slightly in x with time. There will be a comparatively negligible z separation and no y separation. Gravity was included in all computer simulations.

C. Phase Difference Generation

The Converter. Since $\Delta\phi$ is negligible in the open box accelerator it is necessary to convert Δx_a to a potential energy difference which generates phase in the drift space. This is accomplished by what we call the gravitational amplifier; Fig. 2. Here after t_a seconds of electrical acceleration a 10 cm y-length section of the floor of the accelerator is tilted 0.01 rad clockwise so the UCN drift to the right past the edge of a ceiling slot. There they rise into a drift space, in the process hitting a 45° mirror. The mirror converts Δx_a to Δz , an extra gravitational deceleration distance for one spin state, always the same one. That in turn produces a $\Delta v_x = g\Delta z_{initial}/v_x$, ~ 100 times the velocity difference in the accelerator, and a gravitational potential energy difference $\Delta V = mg\Delta z$ between the spin states which will lead to a detectable phase difference in the drift space [Eq. (1)]. Note that the ΔV , proportional to μ_e , arises from the gravitational field acting on the “large” neutron mass after an electric field gradient acts on the tiny electric dipole. This increase in ΔV by $\sim 10^3$ accounts for the increased rate of phase gain after the mirror.

The drift space for practical reasons can only be 10 cm or so long in x but x-reflection on closed gates or fixed walls does not reverse the phase gain, unlike the case in the open box where Δv_x does not reverse when v_x does. This phase gain will be continuous and proportional to the time t_d the UCN is in the drift space. As in the case of the simple interferometer of Sect. II-A, the field, in this case gravity, is conservative so Eq. (1) [$\hbar\Delta\phi = -\int_0^{t_a} \Delta V dt$] applies with limits those of t_d . Because of the parabolic paths ΔV fluctuates, even in sign when the (z,t) trajectories cross, but $\Delta\phi$ gains without changing sign, as shown in Fig. 4.

Since our fields are conservative,

$$-\Delta T = \Delta V = mg\Delta z. \quad (8)$$

At the 45° mirror

$$\Delta z(\text{initial}) = \Delta x_a. \quad (9)$$

Integrating Eq. (5) over time we have

$$\Delta x_a = (\mu_e t_a^2/m)(\partial E_x/\partial x). \quad (10)$$

Using (8), (9), and (10), and doing the integral in Eq. (1) over the time interval t_d common to all the neutrons, we get

$$\hbar\Delta\phi = 0.67g\mu_e t_d t_a^2 (\partial E_x/\partial x). \quad (11)$$

The factor of 0.67 comes from averaging the varying Δz over the many parabolic bounces of each UCN. A further factor of 2 arises from taking the difference between $\Delta\phi$ of Eq. (11) and the $\Delta\phi$ from another set of measurements with the electric field reversed giving an effective $\Delta\phi$

$$\hbar\Delta\phi_e = 1.3g\mu_e t_d t_a^2 (\partial E_x/\partial x) = . \quad (12)$$

Note that Eq. (12) is independent of v . This is a “white fringe” interferometer. The electric field reversal is very important because it automatically helps to take care of a number of possible sources of error such as a slight error in the timing of the second spin flip or an adventitious magnetic field gradient (Sect. IV-B).

As noted in the introduction there have been objections raised that there is no generation of $\Delta\phi$ in the drift space in our experiment. There is contrary evidence, however, from the Kasevich and Chu [7] experiment which produces a phase shift. Their experiment is like ours in that the potential energy difference is developed along strongly overlapping paths of the two partial waves. Also the Hamiltonian is formally almost identical to ours, $-\hbar^2(\Delta^2/2m) + mgz + \mu_m B$, where B is the external guide field in our case and the internal magnetic field of the sodium atom electrons at the nucleus in Ref. [7]. It is also like ours in that it is energy conservative in the periods when phase differences are being generated during the drift although not conservative when the velocity separation of the partial waves is being produced by the exciting laser pulses. They differ in that their trajectories are linear along g , whereas our trajectories follow parabolas in the xz -plane. Nevertheless we do not expect any adverse consequence of this multi-dimensionality since we have also done a calculation using x and z velocity terms which agrees with the phase from Eq. (1). (Proposed simplified tests of these and other questions are described in section V.)

The Convex Floor Amplifier (CFA). The second type of amplifier is somewhat more complicated but has the advantage of much greater sensitivity. It may well be that systematic errors will make this advantage academic. However, one cannot be certain of this so we believe it is worth considering. In this amplifier (Fig. 2) the open box accelerator, after a period of acceleration, t_a , is transformed to what we call the “convex floor amplifier” by warping the floor, by pressure from underneath, to a 10 cm (x) by 50 cm (y) arc of a y-axis

cylinder. The radius of the convexity would be several hundred m, projecting a few microns above the original plane in the middle. In each of successive bounces on such a floor the two spin states, initially slightly separated in x by the accelerator's electric gradient, will bounce on slightly different slopes and move further apart in x , exponentially. A computer calculation confirms that with a floor having a 300 m radius, the initial Δx will grow about a factor of 3.5 every second (a gain of 500 in 5 s) independent of v_z , for $v_z \gg v_x$, all the while maintaining coherence. The convex floor amplifier achieves a practical Δx value in typically one to two orders less time than the accelerator alone. The dihedral roof, with slopes of 0.006 rad, will still retain for a useful amplifier time almost all UCN that were retained with a flat floor despite the box remaining open in x . The convex floor amplifier's shorter cycle time means more runs, hence more UCN, hence better statistics in a given time.

Table 1 exhibits a comparative example of each type of amplifier. When the convex floor amplifier is used, its gain factor $G^{t_{CFA}}$ is inserted in the right hand side of Eq. (12); here is the gain per sec and t_{CFA} is the time on the convex floor. We have calculated that a permanent convex floor will make the effective electric acceleration time very short because the gain quickly dominates and this time-shortening in turn greatly increases the relative importance of the undesirable $\mathbf{v} \times \mathbf{E}$ effect (see Sect. IV-A.)

To convert the amplified x to a phase difference, at an appropriate time the UCN are made to rise to the gravitational amplifier as described above. On the 45° mirror Δx becomes Δz , thus generating a gravitational potential energy difference $mg\Delta z$ between the paired spin states. The time integral of this ΔV , averaged over their now much shallower parabolic trajectories as they bounce on the floor of the shallow drift space box, generates a phase difference.

The choice of having UCN escaping from the tilted floor upward rather than downward is made to simplify the floor-warping bar and its support. The phase difference growth begins as the UCN leave the 45° mirror, and terminates at td as the neutrons enter the Mach-Zehnder interferometer. As mentioned in the introduction, the beam splitter of the Mach-Zehnder must be a magnetized mirror which reflects one spin state and transmits the other. They are reunited at the non-magnetized recombiner mirror through the interferometer, between the splitter and the recombiner, one spin state must be rotated π radians. The phase difference between the two states is given by the ratio of the counts in the two counters of the Mach-Zehnder in the usual fashion. One measurement should be made with the electric fields in one direction and another with the fields in the opposite direction.

D. The Assembly

We will describe the assembly which uses only the simpler gravitational amplifier. The general management of the UCN would be similar in the case of the convex floor amplifier. The neutrons coming from the source must be x -polarized. They could be led into the open box in the y -direction through a y -mirror gate. It would take about 1s to fill the box. After this the RF-field needed to rotate the spin $\pi/2$ to achieve differential acceleration would be started and run for an appropriate time (a few seconds).

After about 100 seconds in the open box, a 10 cm length (in y) of the floor would be tilted clockwise 0.01 rad. The UCN would rise to the gravitational amplifier through a ceiling slot,

hitting the 45° mirror (Fig. 2). This takes advantage of motion in the y direction to improve transfer efficiency. The operation would take the order of 3 seconds in this case and result in a loss of perhaps 1/3 of the neutrons. Reflection on (yz) planes during the transfer must be avoided.

The environment of this experiment must be a guide field of the order of 10^{-8} T, as uniform as practical. It must be in a vacuum chamber and it must be shielded as well as practical from external magnetic fields. Some details of these requirements are discussed in Sect. IV.

After the second spin flip the UCN are less vulnerable to minor magnetic field irregularities and it would be best to lead them outside the magnetic shield and place the polarimeter there. The point of this is that the polarimeter may need a rather high magnetic field and this could be disruptive inside the shield.

We can now make an estimate of the sensitivity of the proposed instrument, using t_a , t_d and $(\partial E_x/\partial x)$ from the gravitational amplifier column of Table 1 in Eq. (12). In the table we arbitrarily assumed $\mu_e = 10^{-28}$ e.cm, for which we get $\Delta P_e = 0.023$. Could one achieve that accuracy? This of course depends on the number of neutrons that can be counted (and systematic errors, some of which will be discussed later). The number of neutrons which could be counted in one filling should be given by

$$N_c = V_b \rho D L v_s \quad (13)$$

where V_b is the volume of the box, 2500 cm³. ρ is taken as the phase space density of UCN attainable at the Institut Laue-Langevin (ILL) [1], which is 0.0036 cm⁻³ (m/s)⁻³. D is the decay factor, 0.54, for 200 s [13], primarily due to inelastic collisions on the Fomblin surface coating (see Sect. IV-C) and L is the fraction surviving after miscellaneous losses (transfer, counter efficiency etc.), guessed as 0.2. v_s , the velocity space occupied, requires some discussion. It is intended to be an average over the real space volume occupied in the open box. The limiting velocity in x is 0.3 m/s. We believe this should be reduced by a factor of 2 for the average over the box. In the y direction 0-4.5 m/s is usable. A similar analysis of z suggests the limits 3 to 4.5 m/s. All these ranges must be doubled for their negative velocity counterparts. v_s then becomes about 8.1 (m/s)³.

From all this we get $N_c = 7.9$ counts per cycle. While the rate is low it should be noted that the counts are concentrated in the last few seconds of a cycle, the live time of the counter, and should be well above background. We should also explain that we have chosen to use cycle times considerably less (~ 0.2) than optimal for our case to get the counting rate up to practical levels.

The estimated fractional error in the polarization measurement would be $2/(\alpha\sqrt{N})$, where N is the total number of counts, half in each electric field direction. α is a “polarization efficiency” or “fringe visibility” factor (= 0.64 in Ref. 1). In Table I we have calculated the N which would give a statistical error (1s) equal to ΔP_e . Note that this value of N is the same as given by the energy-time uncertainty limit, $\Delta\epsilon\Delta t \geq 2\hbar/(\alpha\sqrt{N})$, where $\Delta\epsilon$ is the relevant energy difference, i.e., the potential energy difference $mg\Delta z$, in the drift space. Actually realizing such a sensitivity is extremely difficult owing to the possible systematic effects, some of which are discussed in Sect. IV.

III. COMPARISON TO THE PRECESSION METHOD

This comparison is clearly arbitrary. We use for the accelerator method the parameters of Column 1 of Table 1 except in the case of the ratio of electric forces, $E_p/(\partial E_x/\partial x)$, which we conservatively estimate as 1.0 at most on the basis of arguments concerning leakage currents in Sect. IV-D. For the precession method we use the parameters of the new ILL experiment [14] that may well improve their sensitivity by an order of magnitude.

For the precession method [1] the minimum measurable EDM given by the statistical limit is

$$\mu_{ep} = \frac{\hbar}{2\alpha_e E_p t_p \sqrt{N_p}}. \quad (14)$$

The corresponding quantity for our method (using the gravitational amplifier) obtained from Eq. (12) and our estimate of the accuracy of our phase difference measurement, $2/(\alpha\sqrt{N_A})$ is

$$\mu_{eA} = \frac{2\hbar}{1.3\alpha e (\partial E_x/\partial x) g t_\alpha^2 t_d^2 \sqrt{N_A}} \quad (15)$$

We assume both methods use the same UCN source and the same overall operating time. The ratios (Precession/Accelerator) of volumes of the two experiments R_v , is $60/2.5 = 24$ [14]. The ratio of retained-velocity spaces, R_{vs} , is estimated as $781/8.1 = 96$. This assumes deuterated polystyrene coatings for the precession experiment and Fomblin for us (Sect. IV-C). The ratio of cycle times, R_c , is $100/200$. Finally, the ratio of surviving fractions of UCN, R_{sf} , we estimate as 3.5. (We added a factor of 2 in favor of the precession method for our losses in an extra transfer operation.) Given these assumptions, $N_A/N_P = R_c/(R_v R_{vs} R_{sf}) = 6.2 \times 10^{-5}$. From Eqs. (19) and (20)

$$\frac{\mu_{eP}}{\mu_{eA}} = \frac{0.33 g t_\alpha^2 t_d (\partial E_x/\partial x) \sqrt{N_A}}{t_p E_p \sqrt{N_P}}. \quad (16)$$

Using $t_d = t_a = t_p = 100$ seconds, we then get

$$\frac{\mu_{eP}}{\mu_{eA}} = 240. \quad (17)$$

i.e. the accelerator method is more sensitive.

IV. PROBLEMS

It would be inappropriate at this time to attempt to discuss in detail the many technological problems that may arise. However we will discuss a few that we believe to be the most troubling sources of systematic error or serious background. The omissions are largely in areas of technology which are common to many experiments, e.g., vacua, vibration control, temperature control, magnetometry and high voltage.

A. The $\mathbf{v} \times \mathbf{E}/c^2$ Effect

The relativistically produced magnetic flux density experienced by neutrons moving relative to an electric field is given by $B = \mathbf{v} \times \mathbf{E}/c_2$ (SI units). Its axially directed gradient $\partial B_x/\partial x = [(v_z \partial E_y/\partial x) - (v_y \partial E_z/\partial x)]/c^2$ generates unwanted differential forces in the x-direction on the bipolarized magnetic dipole moment (MDM) in the accelerator. A major concern in these EDM measurements, as also in the precession method, is the fact that one cannot separate the relatively large $\mathbf{v} \times \mathbf{E}$ force ($\mu_m \partial B_x/\partial x$) from that from the EDM ($\mu_e \partial E_x/\partial x$) by turning off the electric field. The $\mathbf{v} \times \mathbf{E}$ effect must be reduced by careful cancellation. We give here a detailed calculation suggesting that the $\mathbf{v} \times \mathbf{E}$ effect would not limit measurements of an EDM greater than about 2×10^{-30} e.cm.

By the symmetry of our geometry (Fig. 2), E_y is small and can be made more so by guard electrodes so the first term of $\partial B_x/\partial x$ becomes negligible (the v_z bouncing also helps by making $\langle v_z \rangle \rightarrow 0$). E_z is a more serious problem. The measure of its importance relative to the EDM force is the effective $(\partial E_z/\partial x)/(\partial E_x/\partial x)$. This ratio of the gradients felt by the magnetic and electric moments has been calculated for the electrode configuration of Fig. 2 and is shown in Fig. 5 for an x,z section through the open box. Using this in a computer program we estimate that the average of the absolute value of that ratio over the volume traversed by the retained UCN would be about 10^{-3} . This is a small number, but there is a worry here that this calculated number may be spoiled by nonuniformities in the dielectric constants of the top and bottom plates of the stationary box. Making these plates much wider than 10 cm as shown in Fig. 2 should reduce edge effects. (Note that the dihedral ceiling angle would not be extended by more than 5 cm from the midplane however so that UCN which entered the high $\partial E_z/\partial x$ regions would not be retained.) Simple measurements of the dielectric constant of the plates could be made to get some idea of their uniformity. In addition it should be possible, although perhaps difficult, to measure $\partial E_z/\partial x$ directly using a piezoelectric crystal. This would furnish a second check on the plates. This problem of uniformity would probably determine the material used for the plates.

The $\mathbf{v} \times \mathbf{E}$ effect is only important in the accelerator. After that the amplifier quickly raises the energy difference so much that $\mathbf{v} \times \mathbf{E}$ does not matter. The trajectories of the UCN in the box will naturally lead to considerable cancellation of the second term in $\partial B_x/\partial x$, due to scanning of the antisymmetrical $\partial E_z/\partial x$. Using the program for calculating trajectories and $\partial E_z/\partial x$ we have calculated the Δx_α induced by the $\mathbf{v} \times \mathbf{E}$ effect for a wide range of initial conditions that still leave the UCN confined in the 10 cm width of the open box for 100 seconds. The resulting Δx_α varied over a 100:1 range, the largest tending to be those passing through high $(\partial E_z/\partial x)$ regions. The average of the largest 1/4 of the Δx_α from the $\mathbf{v} \times \mathbf{E}$ effect produced approximately the same Δx as an EDM of $\sim 10^{-28}$ e.cm. Since that Δx is of random sign the 18,500 neutrons, we claim could be counted in 5.4 days, allow a measurement of the EDM to $\sim 2 \times 10^{-30}$ e.cm accuracy, as far as the $\mathbf{v} \times \mathbf{E}$ effect is concerned. These results are considerably lower than a random walk approximation in which we took 5 cm steps and in which the force was random but the velocity was allowed to accumulate. In our actual case the forces are not random because they tend to change sign systematically about every two cm. This shows that the systematic cancellations are having a very appreciable effect. The $\mathbf{v} \times \mathbf{E}$ effect on Δx appears to rise linearly with time where the EDM of course goes as t_α^2 .

It is fairly clear from looking at Fig. 5 that the relative size of the $\mathbf{v} \times \mathbf{E}$ effect versus that of the EDM could be reduced by a factor of 10 by reducing the width of the open box from 10 to 5 cm. This would cost a factor of two in volume and two in range of v_x . This in turn would only cause a factor of two loss in sensitivity if background were not a serious problem.

It should be said that the computer programs on the results of which these conclusions are based do not include the dielectric effects of the materials of the ceiling and floor of the open box.

There are several experimental approaches to measuring the $\mathbf{v} \times \mathbf{E}$ effect. One way is to measure the effect on $\Delta\phi$ of reducing v_y by a factor of two. Another is to move the electrodes in by several cm. The percentage increment in the $\mathbf{v} \times \mathbf{E}$ effect would be roughly 2.5 times that of the EDM. One could also change t_a by a factor of 1.4. The EDM effect would change by a factor of two but the $\mathbf{v} \times \mathbf{E}$ by 1.4.

B. Magnetic Fields

(We will discuss magnetic fields due to leakage currents in Sect. IV-D.)

Components. The apparatus will need very good magnetic shielding, perhaps even superconducting shields. Our estimates based on the experience of the EDM group at ILL indicate that conventional magnetic shielding should enable interferometric detection at the 10^{-26} e.cm level, and that the use of superconducting shields might allow reaching substantially lower. Their analyses showed the largest expected systematic effect (spurious EDM) arises from hysteresis in the conventional high permeability shield caused by current pulses as the electric field is reversed. Such small displacement currents would not affect superconducting shielding. To limit a spurious EDM signal to 10^{-28} e.cm their precession method needed a magnetic field difference between the runs with reversed electric field averaged over the months' long duration of the experiment of $0.5 = 10^{-17}$ T. In their experiment they got a shielding factor (SF) of 10^5 which, for example, reduced the field from a 20 cm radius current loop carrying 20 mA at a 2 m distance from their shield to the tolerable level, 10^{-11} T at the shield outer surface. A simple one-layer superconducting shield should give $\text{SF} > 10^8$ even for much larger ambient disturbances. A 2m internal diameter superconducting shield will surely be the most expensive part of the apparatus. A brief discussion of a scheme that may improve superconducting shields appears in Ref. [16].

A guide field of the order of 10^{-8} T will be needed to keep the spins of the UCN oriented. This leads to a Larmor precession of 1.8 radians per second. (ILL uses 180 radians per second.) In principle the phase shift this induces could be ignored since it is nearly the same for all UCN and could be removed by the second $\pi/2$ spin rotation in an appropriate fixed phase relation with the first (Sect. II-A).

Perturbing magnetic fields. In our proposed EDM measurements all sources of non-uniformities in the magnetic field, particularly in the accelerator, lead to unwanted phase differences. They are of serious concern because of the huge ratio of μ_m/μ_e . We believe it is only the x-component of the field which contributes significantly because the UCN are polarized in that direction.

There are two such phase-difference-generating terms of concern. The first gives an increment in the precession rate, hence in $\Delta\phi_p$,

$$\Delta\phi_p = \frac{1}{\hbar} \int_0^{t_a+t_d} 2\mu_m (B_x - \langle B_x \rangle_s) dt. \quad (18)$$

Here $\langle B_x \rangle_s$ is the spatial average of B_x in the accelerator and drift spaces. The second and more serious disturbance is a magnetic gradient term significant only in the accelerator because it produces a Δx_{ag} . The effect of this term is amplified in the gravitational amplifier as is the Δx_a from the EDM. In analogy to Eq. (11),

$$\Delta\phi_g = 0.67 \frac{g\mu_m t_a}{\hbar} \int_a^{t_a} \int_{t_a}^{t_d} \frac{\partial B_x}{\partial x} (dt)^2. \quad (19)$$

Since numerically the gradients and the field non-uniformities are of the same order, the gt_d factor, of the order of 1000, is very dominant, and the precession effects can be ignored. The residual x-directed magnetic gradients may well impose the most severe limit on the attainable EDM sensitivity, beyond the constraints of the $\mathbf{v} \times \mathbf{E}$ effect, even after considering that the phase shifts from magnetic gradients are more easily distinguished from those produced by the EDM, by turning off the electric field.

The different paths taken by the individual UCN will lead to different values of $\Delta\phi_g$ because the gradients are not uniform. This could be a serious problem because polarization, which is what would be measured, is a sinusoidal function of $\Delta\phi_g$ (Fig. 6). The $\Delta\phi_g$ of the ensemble must be confined to about ± 1 rad and centered near $P_x = 0$ on one side of a fringe where P_x is a reasonably linear function of $\Delta\phi_g$. If the standard deviation of the $\Delta\phi_g$ in an ensemble were as much as 5 rad the P_x would be that from an average over several fringes and $|P_x(max)|$ would be very small and hence the slope, which determines the sensitivity to the EDM would also be very small. This would then require an enormous number of UCN to measure the much smaller effect of the EDM with even modest accuracy. If the average value of $\Delta\phi_g$ is appreciable, it may be necessary to adjust the phase of the second spin flip slightly to keep the phase difference centered near zero.

It should be noted that Eq. (24) is probably a random walk since there are likely to be many sign changes of $\partial B_x / \partial x$ scanned in the course of 100 s. It would be a sort of integrated random walk, much as we had with the $\mathbf{v} \times \mathbf{E}$ effect and $\Delta\phi_g$ would grow as t_a , not as the EDM effect which grows as t_a^2 .

There are three possible sources of magnetic gradients; ferromagnetic impurities in the apparatus, external fields penetrating the shield and non-uniformities in the guide field itself. Leakage fields must be limited but no usable shield can be totally closed, hence none is perfect. It may be desirable to have several monitors of the magnetic field outside the shield and when these external fields are beyond some limits, shut the measurements down.

We have done some experimental model studies on the problem of field uniformity of the guide field [16] using a Helmholtz-derived double four-coil, guide-field-generating assembly fitting inside a simulated superconducting shield. The measured field inside the accelerator box was uniform, i.e. its variation was not detectable at a sensitivity of 10^{-4} . B_x calculations on the double four-coil assembly gave an average gradient in the accelerator of 10^{-6} ($\times 10^{-8}$) T/m and the scanning for 100 s by the UCN will, we estimate, reduce the magnetic Δx production by a factor of at least 40, giving an effective gradient of $2.5 \cdot 10^{-16}$ T/m and of random sign for each UCN. 18,500 UCN per batch (Table 1) will reduce the variation of the effective magnetic gradient to 0.7% of $2.5 \cdot 10^{-16} \rightarrow 2 \cdot 10^{-18}$ T/m, hence producing Δx_a (and ΔP_x) equal to that from an EDM of $3 \cdot 10^{-29}$ e.cm. This can be checked by

measurements made with UCN using the techniques described below. (The electric fields must be off, of course.)

Reduction of Effects of Variations. The variation of the magnetic fields can be examined with SQUID gradiometers [17] but the ultimate test will have to be done with UCN. This could be done by measuring P_x as a function of frequency (Fig. 6). If, in measurements at, say, four frequencies giving points 1 radian apart in phase at the second $\pi/2$ flip, one gets P_x near zero at each point this would be a sign of a large range of values of the gradient integrals. Reduction of sensitivity by reducing the time, t_d , by a factor of ~ 5 should help to increase $|P_x(max)|$. But one must eventually remedy the magnetic non-uniformities if one needs the full potential sensitivity to the EDM.

In general there are two approaches to coping with excessive magnetic gradients; diagnosing their origin and reducing them, or, lowering the sensitivity of the apparatus to them relative to the EDM sensitivity without unacceptable loss of the latter. Reversing the guide field will show its influence by use of a SQUID gradiometer. One could discriminate between shield leakage and ferromagnetic impurities by varying the external field.

Changing the 4-coil guide-field assembly [16] to an 8 coil assembly would give a guide field uniformity at least tenfold better, in principle. Whether it would be that good in practical construction is an open question. Gradients this small, 10^{-14} T/m or a field difference of $5 \cdot 10^{-16}$ T over $x = 10$ cm of the open box, on a $\langle B \rangle$ field of 10^{-8} T can be measured by a SQUID gradiometer. The residual gradient effect will have to be assayed by measuring its effect on ΔP_x by UCN polarimetry.

Guide field gradient correction coils in the shield in series with the guide field coils are a possibility for all the guide field gradients of importance. Serious gradients from ferromagnetic inclusions could possibly be handled similarly with independent current sources. The design and test principles are discussed for a simpler case in Ref. [18]. A strong effort should be made to achieve mirror symmetry about the x-midplane in relevant structures.

Increase of the guide field current when one is trying to measure the gradients would probably be helpful. Such increases are limited of course by the danger of thermal expansion owing to heating by the current.

Reduction of the x-length of the accelerator by a factor of two would very likely give a major reduction in the gradients. A serious reduction of the guide field current would reduce the gradients from the guide field of course but such a reduction is limited by the Larmor period increases. The time spent in two spin flips, at least 6 Larmor periods, should be small compared to $(t_a + t_d)$.

Generating sharp, non-adiabatic reversals of the guide field at symmetrically distributed times in each run might be of use. Even one reversal in the middle of a run of $t_a + t_d$ is helpful. (This is equivalent to the “ π ” laser pulse in Ref. [7].) Reversals also make the phase difference less sensitive to the absolute value of the field and so more reproducible from run to run. We believe that reversal, with as high a frequency as depolarization will permit, might reduce the variation in the phase difference generated by the guide field gradients.

Another possible tactic is to increase the length of time in the accelerator, perhaps to $t_a = 500$ s to gain x25 and decrease t_d to 4 s, hence reduce the gain in the amplifier by 25. This would give the EDM the same overall gain but a gain increase relative to that of the magnetic gradients of a factor of 5 because the EDM effect grows as t_a^2 and the magnetic gradient effect grows more like t_a . The penalty is a factor of 2.5 loss in counting rate.

Time variations of the fields must be held to 1 part in 10^5 to avoid smearing out the EDM effect. This is well within the state-of-the-art of current control, but is not trivial. The structure of the coil should be quite stable as it is in a volume of well controlled temperatures and the possible small vibrations should not be dangerous because their effects average out. In general, time variations are much less important than they are in the Ramsey method because our very low Larmor frequency, and hence small number of precession periods, makes our $\Delta\phi$ much less sensitive to magnetic field changes.

C. Reflectivity

Fomblin is a fluorinated dehydrogenated nonvolatile liquid ether which has been shown [19] to reflect UCN with velocities below 4.55 m/s with exceptionally low inelastic collision loss rates ($< 10^{-5}$) enabling UCN trapping lifetimes of the order of 3000 seconds [15]. It is the material of choice for coating all the UCN guide channel and mirror surfaces requiring total specular reflection as it provides an adherent smooth film. It seems likely that it will also improve the specularity of reflections as a coating on less-than-ideally planar or smooth surfaces by filling in voids, thus contributing significantly to cost reduction in producing optical flats.

Fomblin does raise a possible difficulty because it would form menisci at corners. The curved surfaces of the menisci could mix components of velocities such as vx and vz . There are several possible ways of mitigating this. There may be a film thickness great enough for good reflection but too thin to form a meniscus particularly if there were a several micron separation of the orthogonal surfaces at the corner. A more heroic possibility is the use of frozen Fomblin or frozen O_2 surfaces as in a remarkable neutron-lifetime measurement done in Russia [20]. This appears to have worked very well. O_2 gives a lifetime for UCN comparable to Fomblin's and a neutron velocity cutoff substantially higher than Fomblin's.

D. Leakage Currents and Surface Charges

Leakage currents can lead to magnetic field gradients which can accelerate the UCN through their relatively huge MDM. Their effects must be minimized, as in the standard precession EDM measurements, which sets effective limits to the field strengths that can be used. These currents can be measured in sum at the source; tracing their branching paths is more difficult. In general we believe this problem is less serious here than in the precession method. In that method the full voltage is applied across a 20 cm section of insulation which must also function as a bottle wall. In our case the insulators could be >50 cm long and are less constrained by non-electrical requirements. Moreover the leakage paths are relatively remote from the UCN trajectories.

Related effects can arise from the fields and currents due to surface charges and their motion relative to the UCN. These charges are probably minimized by coating the surfaces with the liquid Fomblin which would make them mobile and prevent their buildup. However, it is difficult to be quantitative about this and experimental study is needed. These effects are similar to the $\mathbf{v} \times \mathbf{E}$ effect (Sect. IV-A) in that it is difficult to separate them from the

EDM effect because they both depend on the electric field. They can perhaps be separated by their possible non-linear dependence on field strength.

E. Precision and Stabilization

The other components of the interferometers are standard parts of other UCN experiments such as the precession EDM measurements; polarizing mirrors and foils, plane mirrors, magnetized foils, an RF spin flipper, and detectors, although the demands on precision and stability will surely be more severe.

The specifications of flatness, angular tilt and stability should be less demanding than for light interferometry because the partial waves almost completely overlap. There is some concern that reflections which may slightly interchange velocity components should not significantly affect Δv_x or Δx . However, the coherent bipolarized state essentially ensures this.

F. Gravitational and Sagnac Effects

Avoiding unwanted mixing of v_x and v_z in the UCN trajectories in the gravitational field is simplest if the floors of the accelerator and drift spaces are horizontal. A Fomblin pool floor would help here. As the tiny separation of the partial wave packets is along x in the accelerator, the z separation, hence the gravitational and Sagnac (Coriolis) relative phase shifts are essentially zero at all times. In the drift space the Δz intentionally created at the 45° mirror of the gravitational amplifier will oscillate between variable \pm values with each bounce of the partial wave trajectories on the Fomblin floor as they cross vertically. While $\langle \Delta z \rangle$ is not zero, such Sagnac contributions to the total phase shift produced in the drift space are negligible (10^{-4}) compared to the gravitational acceleration that is amplifying the EDM-generated shift.

G. Decoherence

The possible loss of coherence of the two spin states of a given UCN is of some concern. This would presumably occur at a reflection as it is hard to see what might cause it in a vacuum. It would probably take an inelastic scattering to cause decoherence but almost all such result in an increase of the UCN energy since the UCN are far colder than the apparatus (1 mK vs. at least a few K or, more likely, room temperature). Above several mK the neutrons do not reflect well and are quickly lost. The ILL experiment [1] is somewhat reassuring here. They obtained clearly defined fringes (polarization vs, frequency of the spin-flip field) after 68 seconds in their chamber. This also suggests no other source of significant random variation in phase differences exists at their sensitivity level.

H. Control, Calibration and Alignment Measurements

Systematic errors are probably the major worry in an experiment which purports to be as sensitive as the one proposed here. We obviously cannot anticipate all of them, and perhaps

not even the most serious ones in the absence of actual experiments, but a few remarks beyond what we have said about the $\mathbf{v} \times \mathbf{E}$ and magnetic field effects seem obligatory. If a non-zero effect is found it would be advisable to show that it is independent of the sign of the electric field gradient and linearly dependent on the electric field and the drift time. It should also be quadratically dependent on the time in the accelerator. Some of the variants we have suggested in this paper have possible value as control experiments. For example one could check the effect of varying the sign of the initial polarization or the strength of the guide field or the guide field reversal frequency etc. If a non-zero EDM $>10^{-28}$ e.cm is found, the potentially great sensitivity of the interferometer can be used to check for certain systematic effects. Leakage currents could be checked by reducing the voltage and $\mathbf{v} \times \mathbf{E}$ by reducing t_a to which the $\mathbf{v} \times \mathbf{E}$ and EDM responses are different.

One must also worry, if these extreme levels of sensitivity are reached, if one is not confusing a new physical effect with a systematic error.

An internal monitor on the overall instrument performance is the magnetic moment of the neutron. Coils placed near the accelerator cell can generate known weak magnetic field gradients with spatial configurations similar to the electric gradients. Bipolarized UCN can thus be accelerated by their magnetic moments and put through the entire instrument. A comparison made between the measured and predicted phase shifts will serve to reveal a number of systematic effects distorting the EDM measurements but not those arising from the electric field, i.e. current leakage and $\mathbf{v} \times \mathbf{E}$ effects. Both electric and magnetic acceleration can then be concurrently opposed by varying the coil current and its polarity to seek a null phase shift. This comparison method will calibrate the sensitivity, give the sign of the EDM unambiguously, compensate for any non-linear phase shifts, and allow the maximum sensitivity to be used to give the highest EDM measurement precision.

V. SIMPLIFIED TEST OF THE OPERATING PRINCIPLES

We have noted that preliminary tests of the novel principles of our proposal and of their combination are desirable. The relatively large magnetic moment of the neutron makes possible two such simplified and relatively inexpensive tests, each being a rough measurement of the MDM, using differential acceleration of bipolarized neutrons by a magnetic gradient, and drifting to develop a phase shift. The first, and simplest, tests these principles for (thermal) neutrons (which the Kasevich and Chu experiment [7] has established for sodium atoms). As noted in Sect. II-C, there has been criticism of our claim $\Delta\phi$ grows during our drifting stage.

Linear Drift Space Test (Fig. 7). Horizontally polarized neutrons, $v = 2,000$ m/s, selected either by monochromatization or by time-of-flight measurement of a pulsed source, flow along x, the axis of a long solenoid equipped with y axis $\pi/2$ RF-flipper coils near each end. The solenoid generates a guide field, $B_0 = 10^{-3}$ T. The current in the central region, I-0, is held constant to 0.1%. The currents in the two end regions within the flip coils, A and B, can be (equally) varied, to give $\Delta B = 10^{-5}$ T, to produce magnetic gradients at I and 0. The A flip coil produces the bipolarized state whose MDM is differentially accelerated at I, drifts in the 0.5 m drift space I-0, is decelerated at 0 and is terminated in flip coil B, and thence its polarization is measured. The experiment consists of measuring the polarization shift which is the difference ΔP with ΔB on, minus ΔB off. The initial polarization is set

to zero (± 0.05) by adjusting the solenoid current with ΔB off. With a similar setup, Robert *et al.* [21] have shown interference with metastable hydrogen atoms.

With ΔB on, the polarization changes, due to two effects. The first is the effect of the acceleration at I and the motion through the drift space, I to O. This should give a phase difference calculable from Eq. (3), and a polarization change of $\sin \Delta\phi$. For the parameters we give this yields a polarization change of about 0.45. In addition, there is a smaller polarization change due to the change in precession in the regions A to I and O to B when ΔB is turned on. This is easy to calculate to sufficient accuracy and for the case described produces a polarization change of

$$\left(\frac{\overline{AI} + \overline{OB}}{\overline{IO}} \times \frac{\Delta B}{B_0} \times \int_A^B 2\mu_m B_x dt \right) \approx 0.1. \quad (20)$$

Here \overline{AI} means length from A to I. This correction can be applied to the measured $\Delta\phi$ to yield the effect of the phase generation due to drifting.

Miniaturized UCN Test. The second experiment using UCN would address the same questions plus the retention of UCN in an open box with a dihedral roof and the functioning of a gravitational amplifier and drift space with two active coordinates (x and z). The strong magnetic acceleration of the magnetic moment makes possible a UCN test on a greatly reduced hence cheap (cost \sim a few percent of the real experiment) scale.

The UCN would be retained briefly (~ 1 sec) in a small open box with dihedral ceiling with magnetic gradient coils followed by a gravitational amplifier and ~ 1 sec. drift, then $\pi/2$ flipping and polarization detection, all in a short cycle ~ 2 sec. repeated frequently. This could be done in a small (~ 20 cm) apparatus with simple magnetic shielding and possibly in a 99enclosure. One hours' data accumulation should yield a sufficient test of the agreement of measured and known MDM. A pulsed (chopped) UCN input beam with the applied magnetic gradient turned off (or reversed) on alternate pulses (which are separately recorded) would promote a good statistical subtraction of the phase shift arising from a, possibly varying, ambient magnetic gradient.

It is possible that a considerably cheaper test could be conducted using polarized ^3He [22]. Because the phase space density in ^3He could be enormously greater than that of UCNs, the apparatus could be much smaller and more easily shielded and still have higher counting rates. It also avoids the numerous problems of working at a reactor.

VI. OTHER INTERFEROMETERS

There are several other types of interferometers we have considered. As a warning we will describe a superficially attractive method which does not work. One would introduce a broad spectrum of bipolarized UCN in a toroidal chamber, moving circumferentially (Fig. 8). A concentric, roughly toroidal magnetic guide field keeps the two spins approximately circumferential. The two UCN spin states would be accelerated in opposite circumferential directions as they passed through the electric field gradients at the top and bottom of the figure and nominally could do this indefinitely. Unfortunately the radial gradient of the magnetic field - inherent in its curvature-supplies exactly the opposite acceleration. How can this balance an independent electric field effect? It does so because the relevant

circumferential magnetic acceleration is due to a surprising radial component of the magnetic moment, which component is induced by the electric field acting on the EDM.

VII. CONCLUSIONS

Let us admit that this entire paper is very optimistic as to both the technical and economic limits of an interferometer measurement. However, there is an additional argument for the interferometer that should be mentioned. Systematic errors common to two experiments are usually less serious in the one where the signal has been increased even at the expense of some loss in statistical accuracy. Specific problems of a given experiment can of course affect this generalization drastically. Systematic errors may well dominate future developments of the EDM measurements. We believe this is a promising proposal but some important features are not firmly established. What we are arguing here is that they are worth testing as in Sect. V.

ACKNOWLEDGMENTS

We are deeply indebted for the help we got from the late Leonard Goodman. It is a pleasure to be able to thank Henning Esbensen, Morton Hamermesh, Edward Hinds, Victor Krohn, Murray Peshkin, Norman Ramsey, Helmut Rauch, Jack Uretsky and Samuel Werner for advice and help. We have also benefitted from a paper by S. K. Lamoreaux and R. Golub [23]. One of us (T.D.) wishes to acknowledge the generous support of Argonne National Laboratory as a Special Term Appointment in the Physics Division during the time of the completion of this manuscript.

This work was supported by the U.S. Department of Energy, Nuclear Physics Division, under Contract No. W-31-109-ENG-38.

APPENDIX

This appendix is intended to demonstrate that in the open box accelerator the difference in velocity of the bipolarized states does not change sign when the pair reverses its x-velocity. In Fig. 9 we show the velocity vectors in successive reflections on the dihedral ceiling, the right hand one reversing their x-motion component. Here $\Delta\mathbf{v} = \mathbf{v}_{\rightarrow} - \mathbf{v}_{\leftarrow}$; \mathbf{v}_{\rightarrow} is the velocity of the spin state that is always electrically accelerated to the right and \mathbf{v}_{\leftarrow} the velocity of that always accelerated to the left. The points of reflection of the wave vectors are minutely separated in reality but have been moved together for clarity. The tiny effects of further electric acceleration play a completely insignificant role in the time span of the events described below. The following applies for either direction of motion and for either ceiling slope or for any combination thereof.

The vector triangles \mathbf{v}_{\rightarrow} , \mathbf{v}_{\leftarrow} and $\Delta\mathbf{v}$ for the incident and reflected waves are mirror images reflected in the plane normal to the ceiling. ρ is the angle at any time between the vertical and the incident \mathbf{v}_{\rightarrow} (or \mathbf{v}_{\leftarrow} since they are almost perfectly parallel). \mathbf{v}_{\rightarrow} and \mathbf{v}_{\leftarrow} are almost perpendicular to $\Delta\mathbf{v}$ hence ρ is also the angle between $\Delta\mathbf{v}$ and the horizontal (ρ' for the reflected beam), θ is the dihedral slope angle, 0.006 rad. On reflections not reversing x-motion, e.g., the left one in the figure, it can be seen that the angles I, R and θ are related by $I = \rho - \theta = R = \rho' + \theta$, so $\rho' = \rho - 2\theta$ for waves moving away from the x-midplane of the open box ($x=0$), either to right or left, and $\rho' = \rho + 2\theta$ when moving toward $x = 0$. Hence after n ceiling reflections ($n \leq 6$) when receding from $x = 0$, $\rho'_n = \rho_1 - 2n\theta$ will change sign, therefore the x component of motion will reverse as in the right hand reflection. Before and after reflecting in x, $\mathbf{v}_{\rightarrow} = \mathbf{v}_{\leftarrow} + \Delta\mathbf{v}$ which shows that $\Delta\mathbf{v}$ continues to point right even though the UCN will now move left, i.e., $\Delta\mathbf{v}$ does not reverse when the bipolarized UCN reflects its x motion. As the x-reflection occurs the vectors \mathbf{v}_{\rightarrow} and \mathbf{v}_{\leftarrow} are most nearly vertical so $\Delta\mathbf{v}$ is nearly horizontal, and as the UCN passes $x=0$ the $\Delta\mathbf{v}$ vector tilts at most $2n\theta = 8^\circ$ from horizontal and then the tilt diminishes. At $x=0$ the electric gradient force is briefly reduced at most $(1 - \cos 8^\circ) = 1\%$. The oscillation by $2n\theta$ continues until t_a .

Note that the center of mass of the bipolarized state of the neutron experiences no acceleration in any type of electric or magnetic accelerator with static fields. In both open and closed box accelerators, as each partial wave recrosses any electrical equipotential surface, it will have exactly the same kinetic energy, ignoring gravity, as on previous crossings, i.e., it will have been accelerated and equally decelerated between successive crossings. In the open box it nevertheless can gain Δv_x and Δx with respect to the other partial wave (which will have been decelerated, then accelerated) because the two spin states do not cross such equipotential surfaces at the same instant, having had different $\langle v_x \rangle$.

REFERENCES

* Deceased.

- [1] K.F. Smith *et al.*, Phys. Lett. **B234**, (1990) 191.
- [2] N F. Ramsey, Ann. Rev. Nucl. Part. Sci. **32**, (1982) 211.
- [3] I.S. Altarev *et al.*, JETP Lett. **44**, (1986) 460.
- [4] C.G. Shull and R. Nathans, Phys. Rev. Lett. **19**, (1967) 384.
- [5] J. Anandan, Phys. Rev. Lett. **48**, (1982) 1660.
- [6] M.S. Freedman, M. Peshkin, G. R. Ringo, and T. W. Dombek, Proc. 3rd Int. Symp. Foundations of Quantum Mechanics, Tokyo, Japan (1989), p. 38.
- [7] M. Kasevich and S. Chu, Phys. Rev. Lett. **67**, (1991) 181.
- [8] E.J. Heller and S. Tomsovic, Physics Today, **46**, July (1993) 38.
- [9] J. Summhammer *et al.*, Phys. Rev. A **27**, (1983) 2523.
- [10] G. Badurek, H. Rauch, and J. Summhammer, Phys. Rev. Lett. **51**, (1983) 1015.
- [11] D.M. Greenberger and A. W. Overhauser, Rev. Mod. Phys. **51**, (1979) 43, Eq. (2.17).
- [12] P. Hermann *et al.*, Phys. RevLett. **54**, (1985) 1969.
- [13] J. Schmiedmayer, P. Riehs, J. A. Harvey, and N. W. Hill, Phys. Rev. Lett. **66**, (1991) 1015.
- [14] R. Golub, D. Richardson, and S. Lamoreaux, *Ultra Cold Neutrons* (Adam Hilger, Bristol, England 1991) p. 206.
- [15] W. Mampe *et al.*, Phys. Rev. Lett. **63**, (1989) 593.
- [16] M.S. Freedman, G.R. Ringo, and T.W. Dombek, Argonne National Laboratory Physics Division Report No. PHY-8333-HI-96, Dec. 1990, *Some Problems in the Technology of Measurement of the Electric Dipole Moment of the Neutron*.
- [17] S.J. Swithenby, J. Phys. E **13**, (1980) 801.
- [18] M.S. Freedman *et al.*, J. App. Phys. **38**, (1967) 1856.
- [19] J C. Bates, Nucl. Instr. Meth. **216**, (1983) 535.
- [20] A.G. Karitonov *et al.*, in Proc. of III Int. Symp. on Weak and Electromagnetic Interactions in Nuclei, edited by Ts. D. Vylov, (World Scientific, Singapore 1993) p. 70.
- [21] J. Robert *et al.*, Europhys. Lett. **16** (1991) 29.
- [22] E.A. Hinds, private communication.
- [23] S. K. Lamoreaux and R. Golub, nucl-ex/9901007.

TABLES

TABLE I. Parameters of the Interferometers.

	Electrode Potential Difference	100 kV	
	Electrode Spacing	0.5 m	
	$\partial E_x/\partial x$	1.1×10^6 V/m ²	
	Gravitational Amplifier	Convex Floor Amplifier	Units
Assumed EDM	10^{-28}	10^{-28}	e-cm
Assumed t_a	100	15	s
Assumed t_{CFA} *	NA	15	s
Assumed t_d	100	5	s
Δx_a **	1.05	0.024	pm
Δx_d †	0.26	0.31	nm
ΔP_e	0.023	0.027	NA
$(\Sigma t)_c$	200	30	s/cycle
D	0.54	0.91	decay factor
N_c	7.9	13.3	counts/cycle
N	18,500	13,900	total counts
Duration	5.4	0.36	days

*Time in the convex floor amplifier.
** Δx after acceleration.
† Δx after drifting.

FIGURES

FIG. 1. Flow diagram of a simplified (schematic) interferometer. The arrows denote the EDM vectors and their relative orientation and motion (exaggerated). To convert to a more useful assembly (see Fig. 2), the dashed components would be inserted.

FIG. 2. Vertical cross sections of accelerator and amplifiers. The slopes of the dihedral ceiling (and of the floor in the transfer position) are exaggerated. The electrodes are shown at half the distance from the center of the figure they would have in the apparatus. The UCN source, the polarizer and Mach-Zehnder interferometer are not shown.

FIG. 3. Electric fields and gradients in the open box. Units of fields are arbitrary.

FIG. 4. a) The growth of the phase difference (of one of the ensemble of UCN pairs) generated to equal time in the drift space; b), the trajectories of the particular pair of bipolarized UCN which produced the phase difference. Their minute separation is grossly exaggerated. Averaged over the ensemble $\Delta\phi$ grows monotonically; c) the Δz function (magnified) whose time integral generates phase difference.

FIG. 5. $(\partial E_z/\partial x)/(\partial E_x/\partial x)$ from our four electrode array, a measure of the $\mathbf{v} \times \mathbf{E}$ effect versus that of the EDM. The heavy and dotted lines outline part of the open box occupied by the UCN and the contours are isoratio lines. Units are a ratio of 10^{-3} . The shaded areas are all below 1×10^{-3} . Note the antisymmetry.

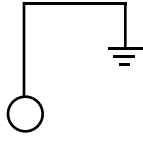
FIG. 6. Idealized “fringe” plots. σ_g is the variance of the magnetic gradient integrals. The $\Delta\phi$ is that after the second spin flip and for a magnetic field of 10^{-8} T and a 200 s time interval between the first and second spin flip, the flips being each $\sim \pi/2$. The RF frequency of the spin flip = 0.29164 Hz.

FIG. 7. Thermal neutron test of differential accelerability of bipolarized neutrons and of phase shift development in the I-O drift space. The accelerating magnetic gradients at I and O are developed by diverting 1.0% of the constant guide field current from the short (0.1 m) ends of the 0.7 m solenoid. The y axis $\pi/2$ RF flipper coils are centered at A and B, 0.6 m apart. Effects due to precession in B_o can be measured by eliminating the field gradient. The RF spin rotation coils can operate continuously.

FIG. 8. The toroidal accelerator. The grounded electrodes carry the low-voltage current for the roughly toroidal guide field. The current would be into the plane of the figure in the central electrode and out of the plane in the other two. Two fragments of typical UCN trajectories are shown dotted. The plane of the figure is horizontal.

FIG. 9. Diagram in velocity space showing on the left a typical reflection on the ceiling and on the right a reflection where v_x reverses. Note that on the right the primed (reflected) velocities from the tilted ceiling represent leftward motion. θ is shown increased by a factor ~ 25 ; $\Delta \mathbf{v}$ and $\Delta \mathbf{v}'$ are increased by many orders of magnitude. The dashed triangle shows what the reflection would have been from a horizontal ceiling. Variables are defined in the text. Note also the progressive leveling of $\Delta \mathbf{v}$ toward the right.

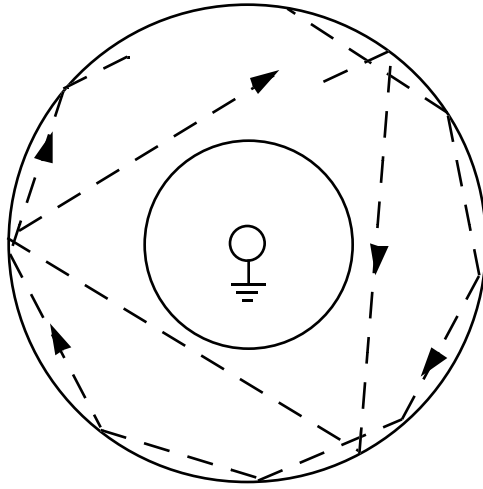
100 KV



100 KV



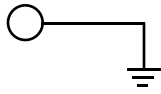
100 KV



100 KV



100 KV



100 KV



